



Sea surface temperature anomalies related to the Antarctic sea ice extent variability in the past four decades

Lejiang Yu¹ · Shiyuan Zhong² · Cuijuan Sui³ · Bo Sun¹

Received: 11 January 2023 / Accepted: 27 December 2023 / Published online: 9 January 2024
© The Author(s), under exclusive licence to Springer-Verlag GmbH Austria, part of Springer Nature 2024

Abstract

The Antarctic sea ice extent, though varying considerably with season and region, had been on a slight increasing trend from late 1970s until mid-2010s when the trend was suddenly reversed. The sea surface temperature anomalies related to the multi-decadal expansion and recent contraction in the Antarctic sea ice extent remain to be uncovered. Here, we demonstrate that the variations in the Antarctic sea ice extent from 1979 through 2020, including the abrupt change in direction that occurred in mid-2010's, can be explained at least partially by the sea surface temperature (SST) oscillations in the Pacific and Atlantic Oceans. Specifically, we show that the changes in the Antarctic sea ice extent are significantly correlated with the Interdecadal Pacific Oscillation (IPO) in all seasons and to the Atlantic Multidecadal Oscillation (AMO) in austral winter and spring. We further demonstrate that SST anomalies trigger planetary wavetrains of different magnitudes and propagating paths depending on seasons. These planetary wavetrains induce anomalous atmospheric circulations over the Southern Ocean that, through transport and melting/freezing, ultimately change sea ice extent.

1 Introduction

One of the most interesting topics regarding polar climate change is the sudden reversal of the Antarctic sea ice extent from a slow expansion that lasted more than three decades starting in late 1970s to a rapid contraction since the mid-2010s (Parkinson 2019). Sea ice cover directly influences not only the ice shelf (Massom et al. 2018) and ecosystem (Labrousse et al. 2017) locally in Antarctica, but also global ocean circulations (Heuzé 2021), ocean-atmosphere heat, moisture and momentum exchanges (Yu 2019), and ocean carbon uptake (Gupta et al. 2020). Consequently, changes in the Antarctic sea ice extent have significant implications that go far beyond the Antarctic region.

Numerous studies have examined the increasing trend in Antarctic sea ice extent and have attributed the increase to

anthropogenic forcing, notably increased greenhouse gas emission and stratospheric ozone depletion, and to natural forcing that arises primarily from sea surface temperature (SST) oscillations. The latter include global-scale oscillations in the Pacific or the Atlantic Oceans, particularly the Pacific Decadal Oscillation (PDO), the Interdecadal Pacific Oscillation (IPO), and the Atlantic Multidecadal Oscillation (AMO) (Li et al. 2014; Meehl et al. 2016; Yu et al. 2017; Yu et al. 2022a), the Zonal Wave Three (ZW3) (Raphael 2007) and the South Pacific Oscillation (Yu et al. 2021), as well as oscillations, such as the Antarctic Oscillation (AAO) or the Southern Annular Mode (SAM) (Thompson et al. 2011; Yu et al. 2023) and the Amundsen Sea Low (ASL) (Raphael et al. 2017), which are more local to the Antarctic. Other important local factors, e.g., local wind patterns (Holland and Kwok 2012), ocean-ice interactions (Zhang 2007; Goosse and Zunz 2014), and freshwater input (Bintanja et al. 2013, 2015), have also been identified to affect Antarctic sea ice cover. The complex interactions among forces of different nature and scales render a complete explanation of the increasing trends in the Antarctic sea ice extent elusive (Hobbs et al. 2016).

Compare to our knowledge about the mechanisms for the increasing trend in the Antarctic sea ice extent in the three decades prior to the mid-2010s, less is known about the forces behind the decreases in recent years. Eayrs et al. (2021) provided a summary of the mechanisms proposed

✉ Cuijuan Sui
suicj@nmefc.cn

¹ MNR Key Laboratory for Polar Science, Polar Research Institute of China, Shanghai, China

² Department of Geography, Environment and Spatial Sciences, Michigan State University, East Lansing, MI, USA

³ Key Laboratory of Marine Hazards Forecasting, National Marine Environmental Forecasting Center, Ministry of Natural Resources, Beijing, China

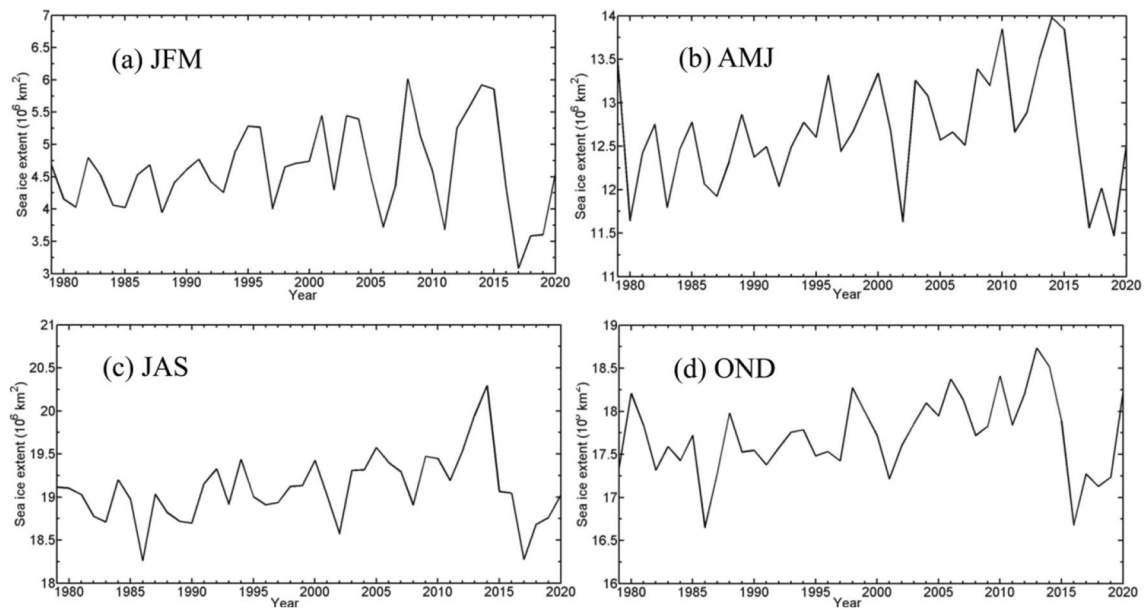
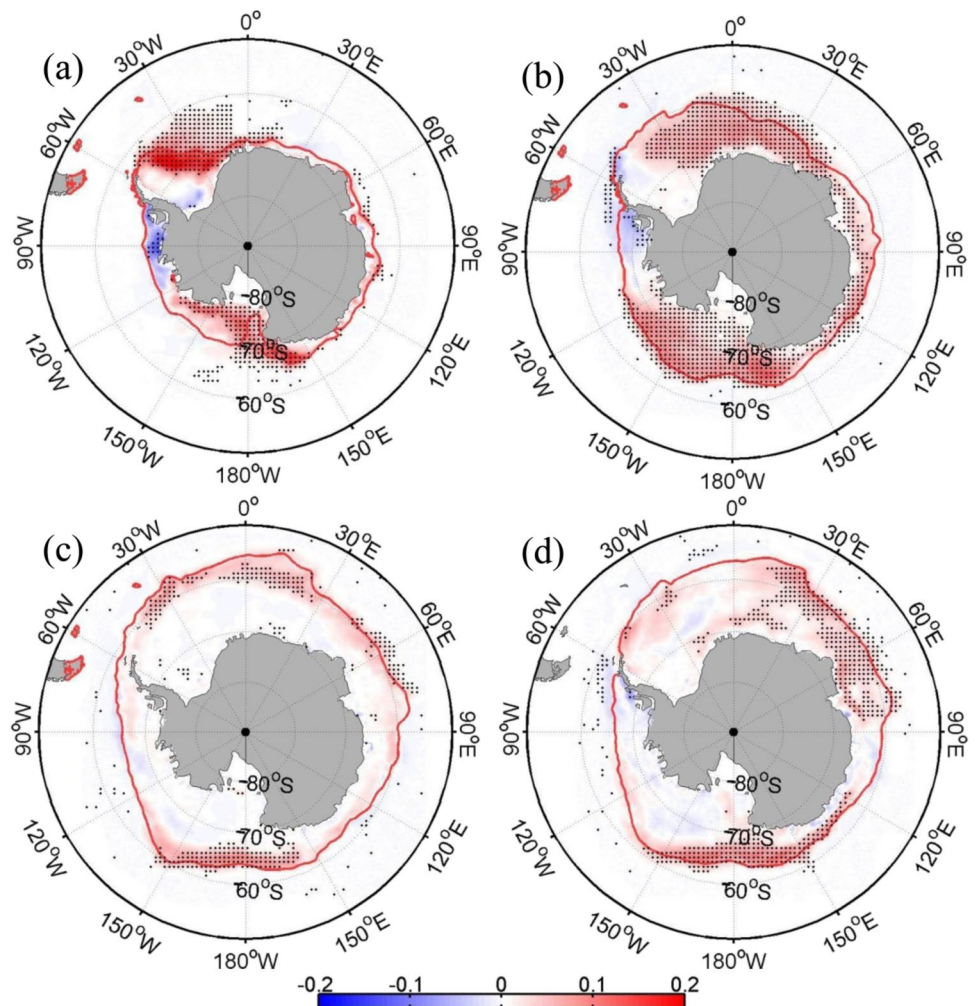


Fig. 1 The time series of Antarctic sea ice extent for the 1979–2020 period in austral summer (JFM) (a), autumn (AMJ) (b), winter (JAS) (c), and spring (OND) (d)

Fig. 2 Regression maps of Antarctic sea ice concentration onto the time series of normalized Antarctic sea ice extent for austral summer (a), autumn (b), winter (c), and spring (d) for the 1979–2020 period. Dotted regions indicate the above 95% confidence level. The thick red lines indicate the Antarctic sea ice extent (sea ice concentration is equal to 0.15)



to explain the recent decline in the Antarctic sea ice extent, which included the teleconnection to SST anomalies in the tropical oceans (Stuecker et al. 2017; Wang et al. 2019; Yu et al. 2022b; Bonan et al. 2023; Zhang and Li 2023) and the southern high-latitude ocean and atmosphere circulation anomalies (Turner et al. 2017; Schlosser et al. 2018; Meehl et al. 2019; Wang et al. 2022; Turner et al. 2022; Yadav et al. 2022; Zhang et al. 2022; Purich and Doddridge 2023; Wang et al. 2023). Wang et al. (2019) also identified the Antarctic stratospheric polar vortex anomalies as a contributor to the Antarctic sea ice anomalies in 2016 (Wang et al. 2019).

Previous studies about the Antarctic sea ice extent have focused on SST role in either the increasing period prior to the mid-2010's or the decreasing period in recent years. What is SST role for the recent four decades including two periods remains to be solved. In the following, we seek for global SST and atmospheric circulations associated with Antarctic sea ice variations for 1979 through 2020.

2 Dataset and methods

The monthly Antarctic sea ice concentration data are available from the US National Snow & Ice Data Center (NSIDC) for the 1979–2020 period (Cavalieri et al. 1996). The sea ice extent is defined as the sum of the areas in the 25 km × 25 km polar stereographic grid cells with sea ice concentration of at least 15%. Monthly sea ice anomalies in are calculated as the subtraction the 42-year average of the monthly data for each month from the original monthly data. The anomalous atmospheric circulations related to the Antarctic sea ice anomalies are from the European Centre for Medium Range Weather Forecasts (ECMWF) fifth generation reanalysis (ERA5) (Hersbach et al. 2020); the ERA5 dataset has a good performance of representing the atmospheric conditions over the Antarctic continent and the Southern Ocean than other contemporary reanalysis datasets (Gossart et al. 2019; Tetzner et al. 2019; Dong et al. 2020).

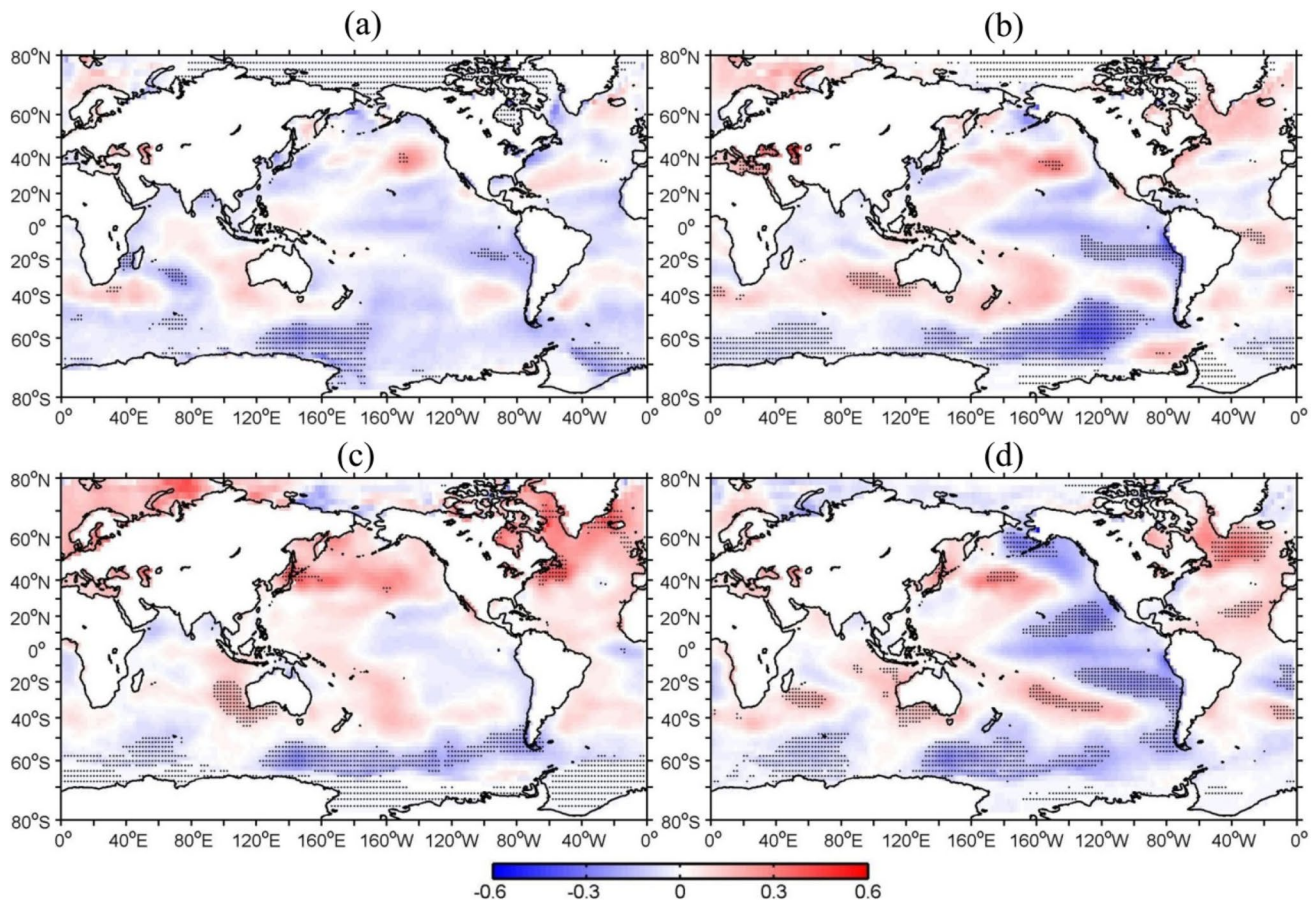


Fig. 3 The same as Fig. 2, but for SST anomalies (°C)

Specific atmospheric variables include mean sea level pressure (MSLP), 2-m air temperature, 10-m wind field, surface downward longwave radiation, and 200-hPa geopotential height and wind. Another important variable in the analysis is the top-of-the-atmosphere outgoing longwave radiation (OLR) obtained from the US National Oceanic and Atmospheric Administration (NOAA) Interpolated OLR dataset (Liebmann and Smith 1996; Henley et al. 2015). In addition to these atmospheric variables, SST anomalies are derived from NOAA's Extended Reconstructed SST V5 (Huang et al. 2017).

The anomalous SST and atmospheric circulations related to Antarctic sea ice anomalies are analyzed through regression analysis. The level of statistical significance is estimated by the Student's *t*-test. Furthermore, the Rossby wave source (RWS) suggested by Sardeshmukh and Hoskins (1988) and wave activity flux (WAF) defined in Takaya and Nakamura (2001) are evoked to demonstrate the generation and propagation of planetary waves, respectively. Finally, the monthly AMO Index (Enfield et al. 2001) is obtained from the US National Center for Atmospheric Research (NCAR) Climate Data Guide and the IPO Index (Power et al. 1999) is obtained from NOAA's Physical Sciences Laboratory database.

3 Results

As shown in Fig. 1 and similar to the results of previous studies (Parkinson 2019), the overall Antarctic sea ice extent shows a slightly upward trend for three and a half decades beginning in 1979 when satellite observations became widely available, and a sharp downward trend since 2014 (2013 for spring). The rates of increase prior are 2.4 , 2.9 , 2.2 , and $2.2 \times 10^4 \text{ km}^2 \text{ yr}^{-1}$ ($p < 0.05$) for austral summer, autumn, winter, and spring, respectively. The rates of declining in recent years are an order of magnitude larger, at -3.3 , -3.5 , -1.7 , and $-1.4 \times 10^5 \text{ km}^2 \text{ yr}^{-1}$, for the corresponding seasons ($p > 0.05$).

Through regression analysis, we show that these trends, including the recent reversal, are largely consistent with the changes in the atmospheric circulation patterns and the anticipated response of sea ice to the dynamical and thermodynamic effects associated with these circulations. We further demonstrate that the changes in the atmospheric circulation patterns are related to SST anomalies through the generation of planetary waves of different amplitudes that propagate along different paths depending on seasons.

To explain Antarctic sea ice extent change, we examine the regression patterns of the sea ice concentration anomaly

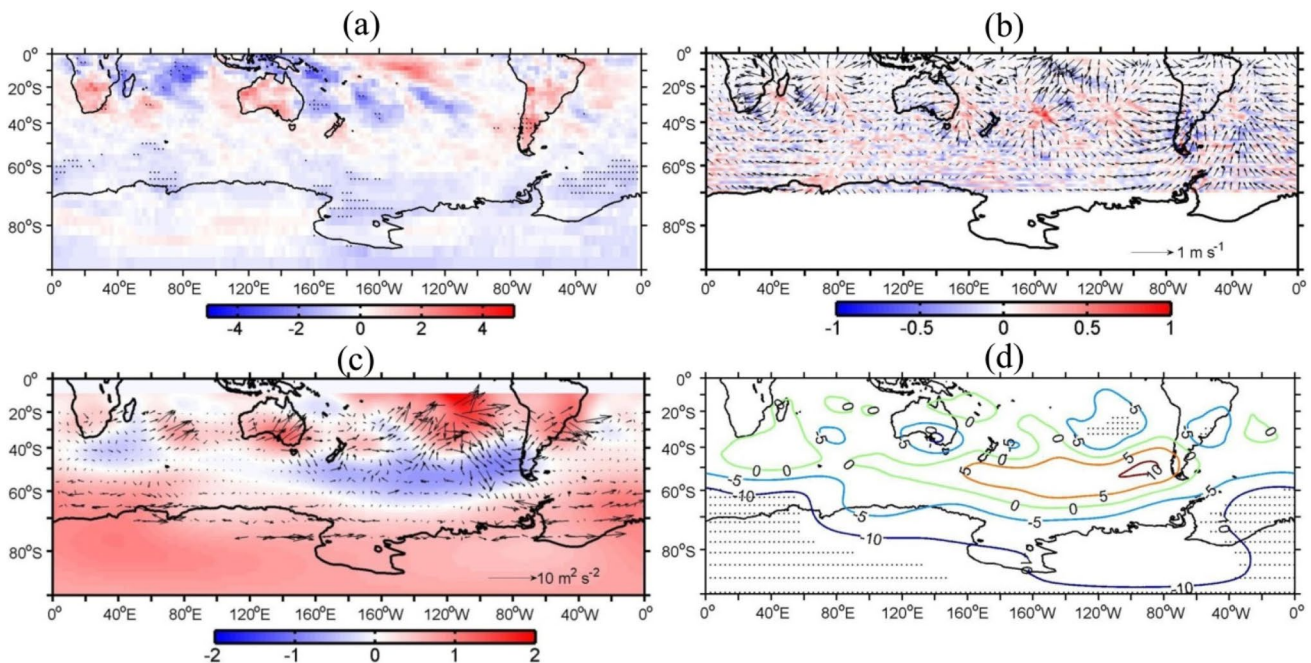


Fig. 4 Regression map of OLR (W m^{-2}) (a), 200-hPa divergent wind (vectors) and Rossby wave source (RWS) (10^{-10} s^{-2}) (b), stream function ($10^7 \text{ m}^2 \text{ s}^{-1}$) and wave activity flux (WAF) (vectors) (c), and

200-hPa geopotential height (gpm) (d) onto the time series of normalized Antarctic sea ice extent for austral summer. Dotted regions in panels (a) and (d) denote above 95% confidence level

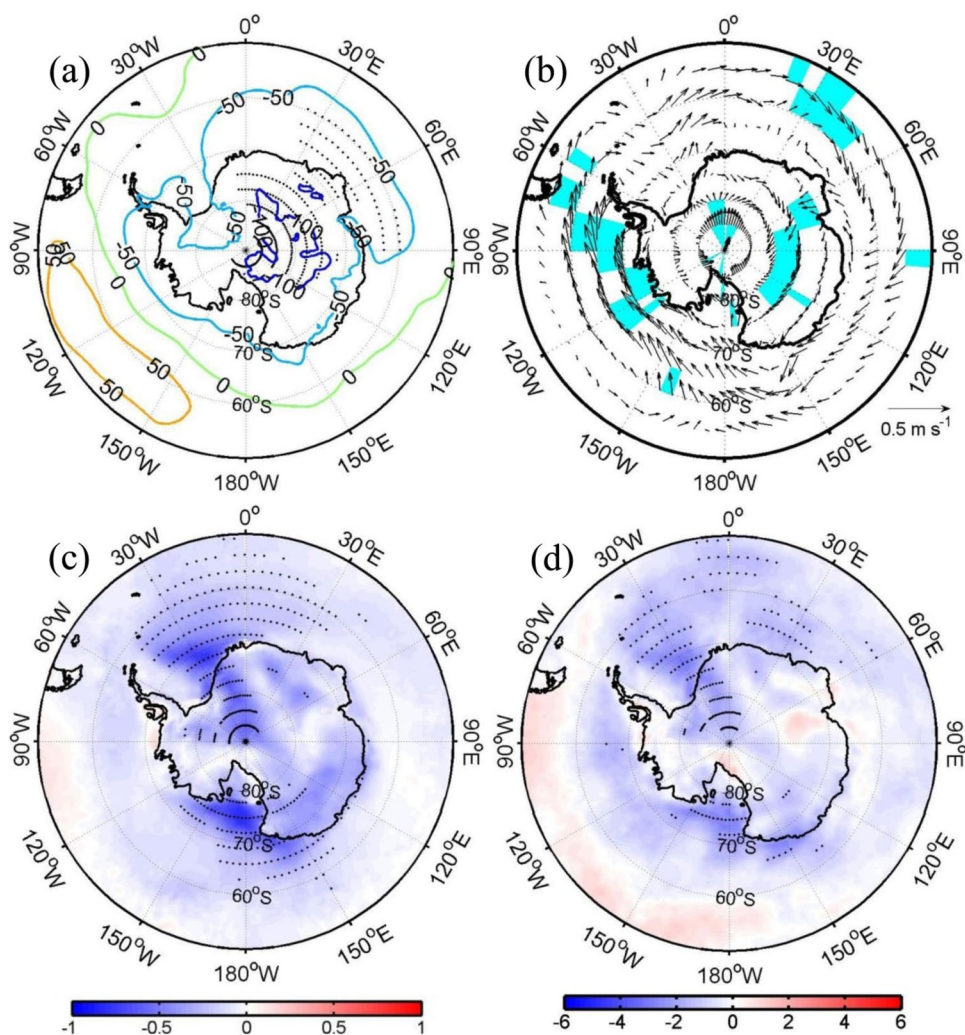
field onto the time series of normalized Antarctic sea ice extent, calculated as the time series of anomalous Antarctic sea ice extent divided by its standard deviation. The spatial regression patterns shown in Fig. 2 correspond to a positive slope or increasing trend with magnitude of one standard deviation of the sea ice extent. Negative slopes of the same magnitude are represented by the inverted patterns (not shown).

For austral summer, positive sea ice concentration anomalies prevail across the Southern Ocean with the exception of the Bellingshausen Sea and southwestern Weddell Sea. The pattern is similar for austral autumn, but the areas of positive anomalies are somewhat larger and the areas of negative sea ice anomalies have also expanded to include the northeast part of the Antarctic Peninsula. Austral winter and spring are characterized by positive sea ice anomalies over most of the Southern Ocean.

Previous studies have suggested the existence of a teleconnection between the Antarctic sea ice anomalies and

the global SST anomalies (Li et al. 2014; Meehl et al. 2016; Yu et al. 2017; Yu et al. 2022a). To explore this teleconnection, we show in Fig. 3 the spatial regression patterns of the anomalous SST onto the time series of normalized sea ice extent. The SST regression patterns, which correspond to the sea ice regression patterns (Fig. 2), are characterized by a prominent IPO signal (negative phase) in austral autumn and spring, with negative SST anomalies in the tropical central and eastern Pacific Ocean flanked by positive SST anomalies in both the central and the tropical western Pacific Ocean. A positive phase AMO is also noticeable, but only in austral winter and spring. The 10-year filtered IPO index and the time series of the Antarctic sea ice extent anomalies are inversely correlated, with the correlation coefficients varying by season, at -0.59 ($p < 0.01$) for austral summer, -0.40 ($p < 0.05$) for austral autumn, -0.47 ($p < 0.02$) for austral winter, and -0.68 ($p < 0.01$) for austral spring. The 10-year filter is applied to obtain the decadal and interdecadal signal in the IPO index. Similarly, significant correlations are also found

Fig. 5 Regression map of **a** mean sea level pressure (Pascal), **b** 10-m wind field (vectors), **c** 2-m air temperature ($^{\circ}\text{C}$), and **d** surface downward longwave radiation (10^5 W s^{-1}), onto the time series of normalized Antarctic sea ice extent for austral summer (JFM). Dotted in panels (a), (c), (d) and shaded in panel (b) regions indicate above 95% confidence level



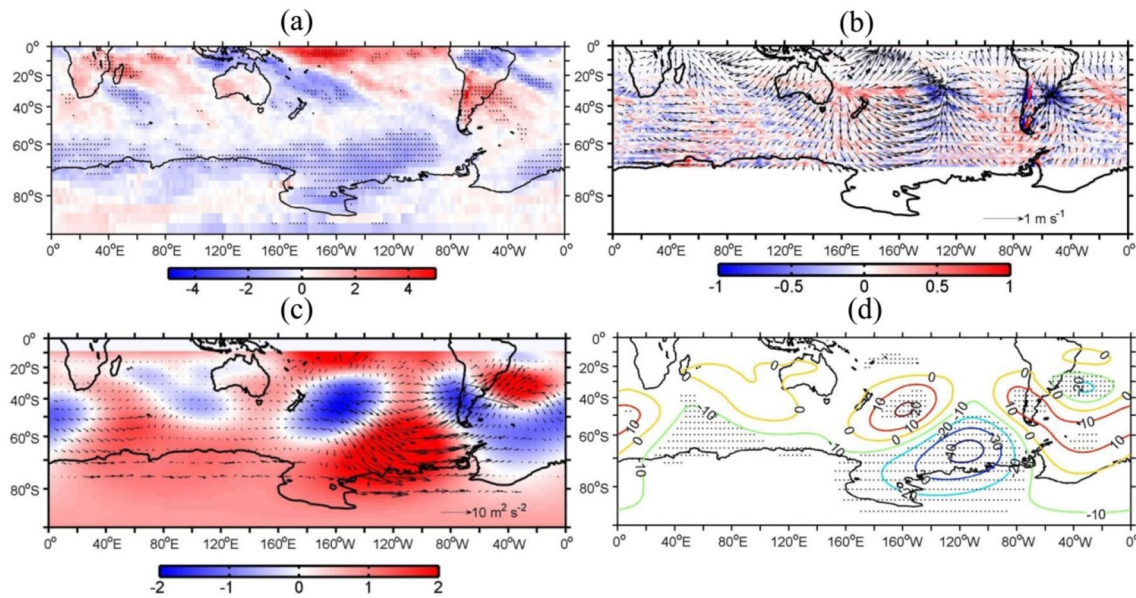
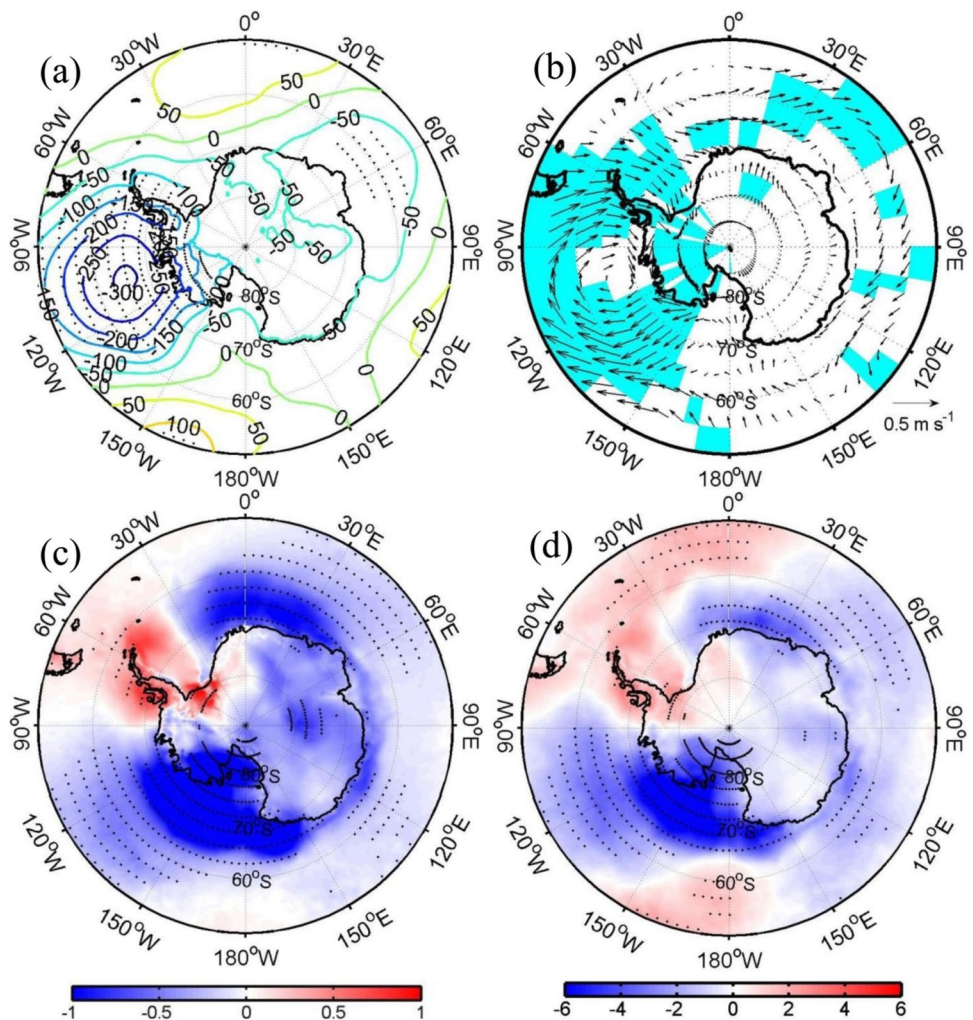


Fig. 6 Regression map of OLR (W m^{-2}) (a), 200-hPa divergent wind (vectors) and Rossby wave source (RWS) (10^{-10} s^{-2}) (b), stream function ($10^7 \text{ m}^2 \text{ s}^{-1}$) and wave activity flux (WAF) (vectors) (c), and

200-hPa geopotential height (gpm) (d) onto the time series of normalized Antarctic sea ice extent for austral autumn. Dotted regions in panels (a) and (d) denote above 95% confidence level

Fig. 7 Regression map of a mean sea level pressure (Pascal), b 10-m wind field (vectors), c 2-m air temperature ($^{\circ}\text{C}$), and d surface downward longwave radiation (10^5 W s^{-1}), onto the time series of normalized Antarctic sea ice extent for austral autumn. Dotted in panels (a), (c), (d) and shaded in panel (b) regions indicate above 95% confidence level



between the 10-year filtered AMO index and the normalized time series of Antarctic sea ice extent for austral winter (0.53, $p < 0.01$) and spring (0.56, $p < 0.01$).

To explore the physical processes behind the statistically significant correlations between the anomalous SST and the Antarctic sea ice concentration patterns corresponding to sea ice extent, we turn our attention to the spatial regression patterns of the anomalous atmospheric circulation variables (Figs. 4, 5, and 6). For austral summer, negative OLR anomalies (Fig. 4a) appear over the tropical western Pacific Ocean indicating enhanced convection as a result of the positive SST anomalies (Fig. 3a) in the region. The deep convections generate or strengthen 200-hPa divergent wind and positive RWS (Fig. 4b) over the southwestern Pacific Ocean. An anomalous Rossby wavetrain propagates eastwards into the eastern Pacific and then southeastwards into the Bellingshausen Sea (Fig. 4c and d). The wavetrain is related to the positive 200-hPa height anomalies over the southeastern Pacific Ocean, in contrast to negative anomalies over the southern high-latitude regions (Fig. 4d). The pattern of the MSLP anomalies, which is similar to that of the anomalous 200-hPa height, resembles a positive phase of the SAM (Fig. 5a). The positive SAM index is associated with stronger westerly winds (Fig. 5b) and decreased surface air temperature and downward longwave radiation across the Southern Ocean with the exception of the Bellingshausen Sea (Fig. 5c and d). These near-surface wind, temperature, and radiation patterns resemble those of anomalous sea ice pattern. Lower temperature/radiation corresponds to positive sea ice anomalies, and vice versa (Li et al. 2014).

For austral autumn, negative OLR anomalies induced by positive SST anomalies in the southwestern Pacific Ocean produce positive 200 hPa divergence wind and RWS (Fig. 6a–d) (Fig. 3b). An anomalous Rossby wavetrain triggered by the positive RWS propagates southeastwards into the Amundsen and Bellingshausen Seas and then into the southern Atlantic Ocean (Fig. 6c and d). The anomalous 200-hPa heights (Fig. 6d) display a negative phase of the Pacific South America (PSA) mode (Mo and Higgins 1998), which has been shown to influence the climate of West Antarctica as suggested by Mo and Paegle (2001). The significantly negative MSLP anomalies in the Amundsen and Bellingshausen Seas strengthens the Amundsen Sea Low (ASL) (Fig. 7a), which generate anomalous northerly winds over the Bellingshausen and western Weddell Seas and southerly winds over the Amundsen and Ross Seas (Fig. 7b). The positive MSLP anomalies induce southwesterly winds over the southern Atlantic Ocean. From the dynamic perspective, anomalous southerly (northerly) winds push sea ice offshore (onshore), which increase (decrease) sea ice extent. From the thermodynamic perspective, positive downward longwave radiation anomalies favor increased surface air temperature and reduced sea ice cover over the Bellingshausen and western Weddell Seas, while the opposite occurs across the rest of the Southern Ocean (Fig. 7c and d). For austral winter, a Rossby wavetrain appears over the tropical western Pacific Ocean where positive RWS exists due to enhanced convection (Fig. 8a and b) by the positive SST anomalies in the region (Fig. 3c). The wavetrain splits into two branches, with one branch propagating southeastwards into West Antarctica

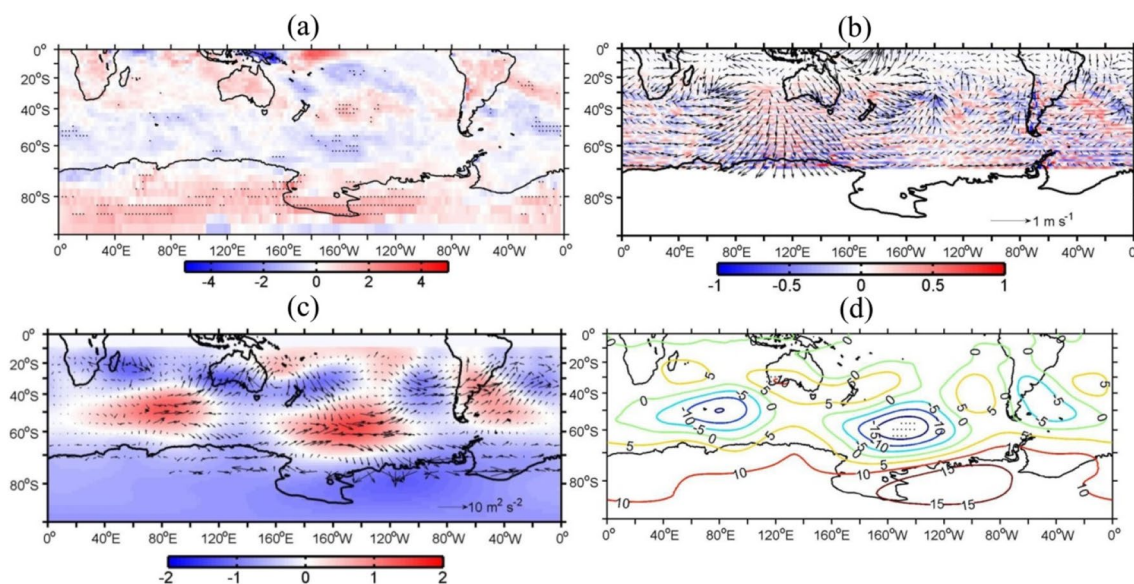


Fig. 8 Regression map of OLR (W m^{-2}) (a), 200-hPa divergent wind (vectors) and Rossby wave source (RWS) (10^{-10} s^{-2}) (b), stream function ($10^7 \text{ m}^2 \text{ s}^{-1}$) and wave activity flux (WAF) (vectors) (c), and

200-hPa geopotential height (gpm) (d) onto the time series of normalized Antarctic sea ice extent for austral winter. Dotted regions in panels (a) and (d) denote above 95% confidence level

Fig. 9 Regression map of **a** mean sea level pressure (Pascal), **b** 10-m wind field (vectors), **c** 2-m air temperature ($^{\circ}\text{C}$), and **d** surface downward longwave radiation (10^8 W s^{-1}), onto the time series of normalized Antarctic sea ice extent for austral winter. Dotted in panels **(a)**, **(c)**, **(d)** and shaded in panel **(b)** regions indicate above 95% confidence level

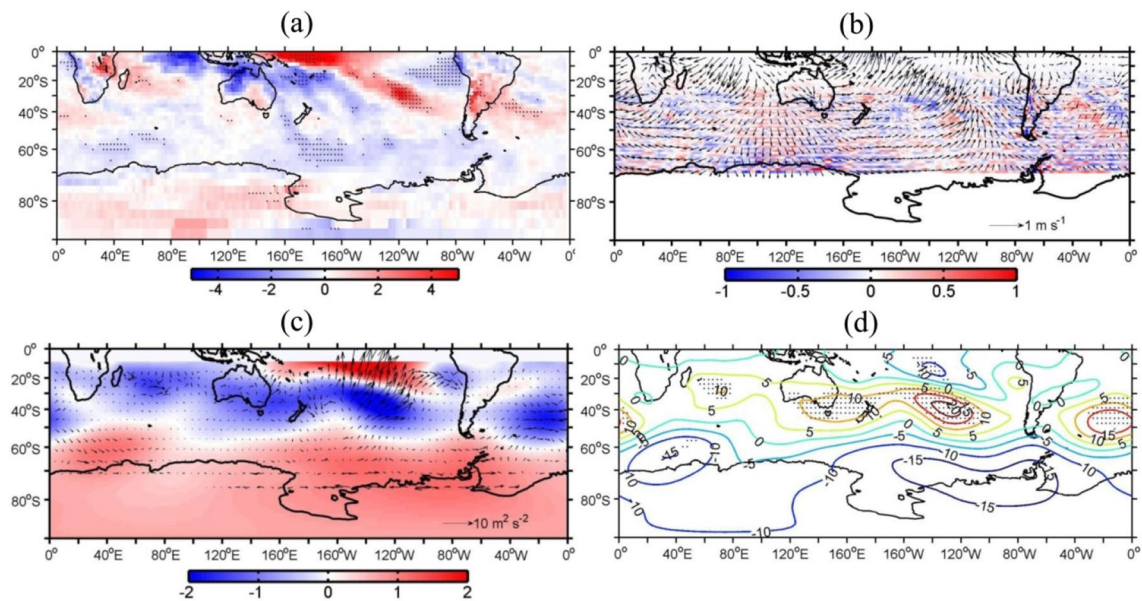
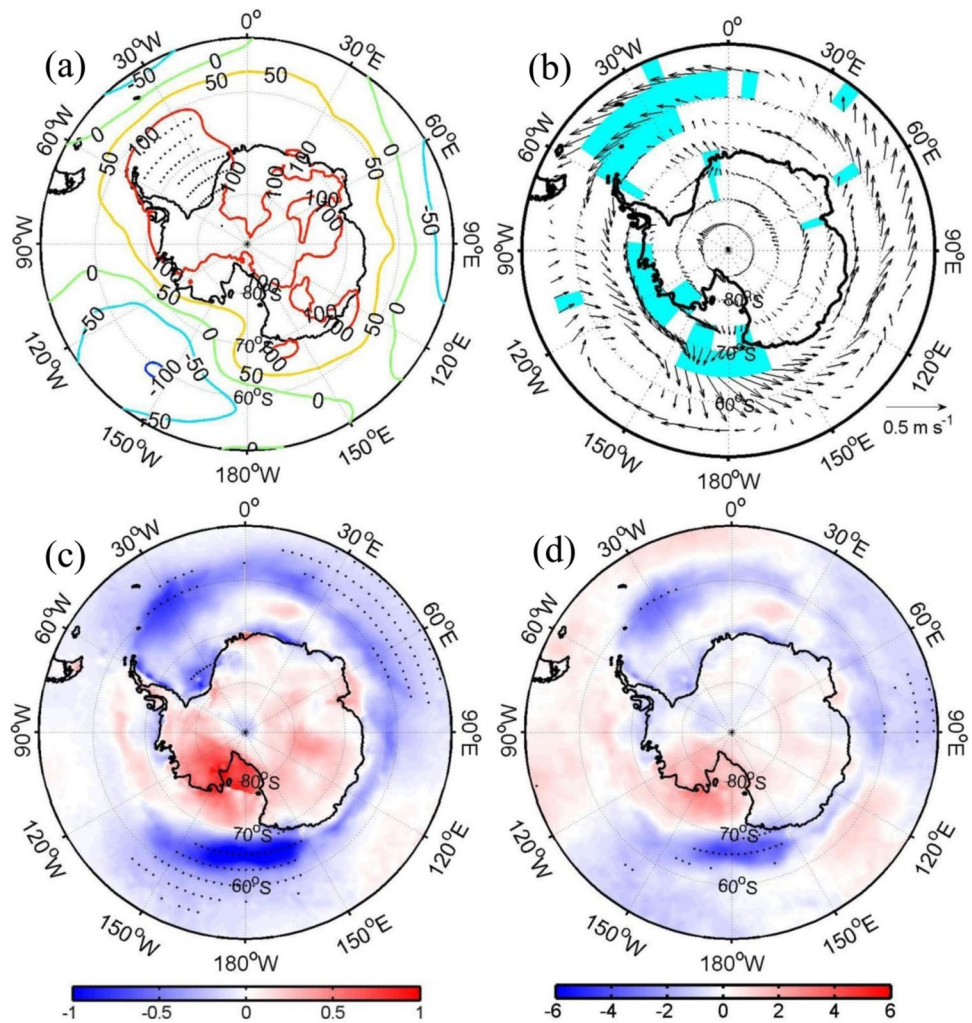


Fig. 10 Regression map of OLR (W m^{-2}) **(a)**, 200-hPa divergent wind (vectors) and Rossby wave source (RWS) (10^{-10} s^{-2}) **(b)**, stream function ($10^7 \text{ m}^2 \text{ s}^{-1}$) and wave activity flux (WAF) (vectors) **(c)**, and

200-hPa geopotential height (gpm) **(d)** onto the time series of normalized Antarctic sea ice extent for austral spring. Dotted regions in panels **(a)** and **(d)** denote above 95% confidence level

and the other propagating eastwards into the eastern Pacific Ocean, South America, and the southern Atlantic Ocean (Fig. 8c and d). Similarly, a wavetrain is generated over the western Indian Ocean, and it propagates southeastwards into the southern Indian Ocean. Afterwards, a branch of the wavetrain reflects back into Australia and the other branch continues to propagate southeastwards into East Antarctica. The two wavetrains result in stronger ASL and positive 200-hPa height and MSLP anomalies over the southern high-latitude regions, with a spatial pattern resembling the negative phase of the SAM (Figs. 8d, 9a). An anomalous

cyclone over the Amundsen and Ross Seas transports sea ice onshore in the Bellingshausen Sea and offshore in the Ross Sea (Fig. 9b). Similarly, the anomalous southerly winds over the Weddell Sea and southeasterly winds over the coast of East Antarctica contribute to the expansion of sea ice cover in these regions. The patterns of surface air temperature and downward longwave radiation anomalies are consistent with the patterns of sea ice anomalies (Fig. 9c, d).

For austral spring, positive 200-hPa divergent wind and RWS appear over the tropical eastern Indian Ocean and the southwestern Pacific Ocean where positive SST anomalies

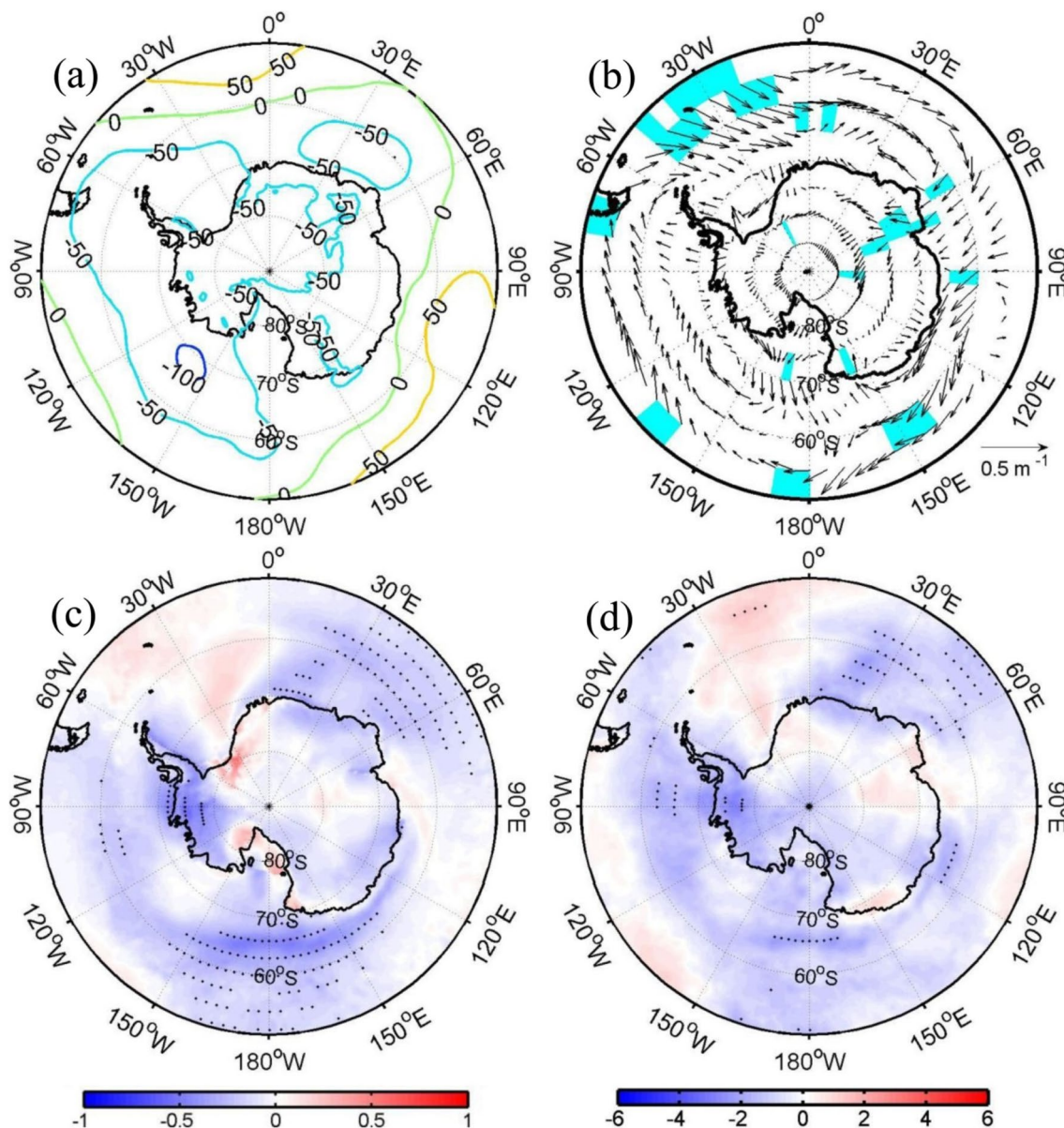


Fig. 11 Regression map of **a** mean sea level pressure (Pascal), **b** 10-m wind field (vectors), **c** 2-m air temperature ($^{\circ}\text{C}$), and **d** surface downward longwave radiation (10^5 W s^{-1}), onto the time series of

normalized Antarctic sea ice extent for austral spring. Dotted in panels (a), (c), (d) and shaded in panel (b) regions indicate above 95% confidence level

(Fig. 3d) boost convection (Fig. 10a, b). An anomalous wavetrain excited over the region to the southeast of Australia propagate southeastwards, but most reflect back into the central and eastern Pacific Ocean (Fig. 10c and d). A small branch of the wavetrain propagates eastwards into the Amundsen and Bellingshausen Seas and the southern Atlantic Ocean. Near the surface, the wavetrain is accompanied by a spatial pattern resembling the positive polarity of the SAM (Figs 10d, 11a), which produces anomalous southerly and southwesterly surface winds (Fig. 11b) and negative surface air temperature and downward longwave radiation anomalies (Fig. 11c and d) in the southwestern Pacific Ocean and thus positive sea ice anomalies in the region. Similarly, over the southern Indian Ocean, the expanded sea ice cover is in accord with the negative surface air temperature and downward radiation anomalies there. The anomalous southwesterly winds over the region of 0–30°E also help the expansion of sea ice there.

4 Conclusion

We have demonstrated, through regression analysis of sea ice, SST and atmospheric data, that the Antarctic sea ice trend from 1979 through 2020, including the abrupt change in direction around 2014, can be largely explained by SST oscillations and the associated anomalous atmospheric circulations over the Pacific and the Atlantic Oceans.

In particular, we show that the Antarctic sea ice changes are closely related to two SST interdecadal variability modes, the IPO in the Pacific Ocean, and the AMO in the Atlantic Ocean. The connection to IPO is significant for all four seasons. However, the connection to AMO is significant only for austral winter and spring. The two modes correspond to different spatial patterns and magnitude of the SST anomalies, which excite planetary wavetrains of different amplitude and propagation path. The differences in the wavetrains induce season-dependent responses in the MSLP fields in the Southern Oceans that are characterized specifically by positive phase of the SAM for austral summer and spring, negative phase of the SAM for austral winter, and negative phase of the PSA1 for austral autumn. The patterns of the anomalous surface wind, air temperature, and downward longwave radiation fields corresponding to the anomalous MSLP fields are largely consistent with the anomalous sea ice patterns in different seasons and different regions of the Southern Ocean.

5 Discussion

Previous studies investigated the role of the IPO and AMO in the Antarctic sea ice concentration anomalies during the sea ice expansion period from late 1970s to mid-2010's (Li et al. 2014; Meehl et al. 2016; Yu et al. 2017; Chung et al. 2022). By

extending the period to 2020, the current study reveals that the two interdecadal SST modes are related not only to the slow sea ice expansion prior to 2014, but also to the rapid contraction since then. While the results here show how Antarctic sea ice respond to natural forcing within the climate system, as represented by the two SST modes, it is important to note that external forces, such as anthropogenic greenhouse gas emission and ozone depletion, also play an important role in driving the changes in the Antarctic sea ice extent, especially in austral summer (Sigmond and Fyfe 2010; Bitz and Polvani 2012; Landrum et al. 2017). A serious limitation of the current study is the relatively short time series (42 years) of the atmospheric and oceanic data for adequately capturing the interdecadal signal. In future studies, model data from the Coupled Model Intercomparison Project Phase 6 (CMIP6) and longer-term reanalysis and reconstruction data may be used to confirm and further elucidate the connection between the IPO and AMO indices and the Antarctic sea ice change on interdecadal scale. Idealized numerical experiments using coupled atmosphere and ocean models should also prove useful for such purpose.

Acknowledgements We thank the European Centre for Medium-Range Weather Forecasts (ECMWF) for the ERA5 data. We also acknowledge the help from the two anonymous reviewers in improving the manuscript.

Author contribution LY designed the research, analyzed the data, and wrote the first draft of the paper. SZ revised the first draft and provided useful insights during various stages of the work. CS and BS provided some comments and helped with editing the paper. All authors reviewed the manuscript.

Funding This study is funded by the National Science Foundation of China (41941009), the National Key R&D Program of China (No. 2022YFE0106300), and the fundamental research funds for the Norges Forskningsråd. (No. 328886).

Data Availability All data used in the current analysis are downloadable from public domains. Specifically, the monthly Antarctic sea ice from the US National Snow & Ice Data Center (NSIDC) can be accessed from <http://nsidc.org/data/NSIDC-0051>. ERA5 reanalysis is available at <https://doi.org/10.24381/cds.6860a573>. SST dataset derived from NOAA's Extended Reconstructed SST V5 can be downloaded from <https://www1.ncdc.noaa.gov/pub/data/cmb/ersst/v5/netcdf/>. OLR dataset are derived from https://psl.noaa.gov/data/gridded/data.uninterp_OLR.html. The monthly AMO and IPO indices are obtained from <https://climateguide.ucar.edu/climate-data/atlantic-multi-decadal-oscillation-amo> and <https://psl.noaa.gov/data/timeseries/IPOTPI/>, respectively.

Code availability The MATLAB code used in this paper is available as long as authors are contacted.

Declarations

Ethics approval Ethics approval is not required for this study.

Consent to participate Consent to participate is not required for this study.

Consent for publication Consent for publication is not required for this study.

Competing interests The authors declare no competing interests.

References

- Bitz CM, Polvani LM (2012) Antarctic climate response to stratospheric ozone depletion in a fine resolution ocean climate model. *Geophys Res Lett* 39:L20705
- Bintanja R, van Oldenborgh GJ, Drijfhout SS, Wouters B, Katsman CA (2013) Important role for ocean warming and increased ice-shelf melt in Antarctic sea-ice expansion. *Nat Geosci* 6:376–379
- Bintanja R, Van Oldenborgh GJ, Katsman CA (2015) The effect of increased fresh water from Antarctic ice shelves on future trends in Antarctic sea ice. *Ann Glaciol* 56:120–126
- Bonan DB, Dörr J, Wills RCJ, Thompson AF, Årthun M (2023) Sources of low-frequency variability in observed Antarctic sea ice. *EGU*sphere [preprint]. <https://doi.org/10.5194/egusphere-2023-750>
- Cavaliere DJ, Parkinson CL, Gloersen P, Zwally HJ (1996) updated yearly. Sea Ice Concentrations from Nimbus-7 SMMR and DMSP SSM/I-SSMIS Passive Microwave Data, Version 1. [Indicate subset used]. NASA National Snow and Ice Data Center Distributed Active Archive Center, Boulder, Colorado USA. <https://doi.org/10.5067/8GQ8LZQVLOVL>
- Chung E-S, Kim S-J, Timmermann A, Ha K-J, Lee S-K, Stuecker MF, Rodgers KB, Lee S-S, Huang L (2022) Antarctic sea-ice expansion and Southern Ocean cooling linked to tropical variability. *Nat Clim Change*. <https://doi.org/10.1038/s41558-022-01339-z>
- Dong X, Wang Y, Hou S, Ding M, Zhang Y (2020) Robustness of the recent global atmospheric reanalyses for Antarctic near-surface wind speed climatology. *J Climate* 33:4027–4043
- Eayrs C, Li X, Raphael MN, Holland DM (2021) Rapid decline in Antarctic sea ice in recent years hints at future change. *Nat Geosci* 14:460–464
- Enfield DB, Mestas-Nuñez AM, Trimble PJ (2001) The Atlantic multidecadal oscillation and its relation to rainfall and river flows in the continental U.S. *Geophys Res Lett* 28:2077–2080
- Gosse H, Zunz V (2014) Decadal trends in the Antarctic sea ice extent ultimately controlled by ice-ocean feedback. *Cryosphere* 8:453–470
- Gossart A, Helsen S, Lenaerts JTM, Broucke SV, van Lipzig NPM, Souverijns N (2019) An evaluation of surface climatology in state-of-the-art reanalyses over the Antarctic ice sheet. *J Climate* 32:6899–6915
- Gupta M, Follows MJ, Lauderdale JM (2020) The effect of Antarctic sea ice on Southern Ocean carbon outgassing: capping versus light attenuation. *Global Biogeochem Cycles* 34:e2019GB006489
- Henley BJ, Gergis J, Karoly DJ, Power SB, Kennedy J, Folland CK (2015) A tripole index for the interdecadal Pacific oscillation. *Climate Dynam* 45:3077–3090. <https://doi.org/10.1007/s00382-015-2525-1>
- Hersbach H, Bell B, Berrisford P, Hirahara S, Horanyi A, Muñoz-Sabater J, Nicolas J, Peubey C, Radu R, Schepers D, Simmons A, Soci C, Abdalla S, Abellan X, Balsamo G, Bechtold P, Biavati G, Bidlot J, Bonavita M et al (2020) The ERA5 global reanalysis. *Q J Roy Meteorol Soc* 146:1999–2049
- Heuzé C (2021) Antarctic bottom water and North Atlantic deep water in CMIP6 models. *Ocean Sci* 17:59–90
- Hobbs WR, Massom R, Stammerjohn S, Reid P, Williams G, Meier W (2016) A review of recent changes in Southern Ocean sea ice, their drivers and forcings. *Global Planet Change* 143:228–250
- Holland PR, Kwok R (2012) Wind-driven trends in Antarctic sea-ice drift. *Nat Geosci* 5:872–875
- Huang B, Thorne PW, Banzon VF, Boyer T, Zhang H-M (2017) Extended reconstructed sea surface temperature version 5 (ERSSTv5), Upgrades, validations, and intercomparisons. *J Climate* 28:911–930
- Labrousse S, Sallée J-B, Fraser AD, Massom RA, Reid P, Hobbs W, Guinet C, Harcourt R, McMahon C, Authier M, Bailleul F, Hindell MA, Charrassin J-B (2017) Variability in sea ice cover and climate elicit sex specific responses in an Antarctic predator. *Sci Rep* 7:43236
- Landrum LL, Holland MM, Raphael MN, Polvani LM (2017) Stratospheric ozone depletion: an unlikely driver of the regional trends in Antarctic sea ice in austral fall in the late twentieth century. *Geophys Res Lett* 44:11,062–11,070
- Li X, Holland DM, Gerber EP, Yoo C (2014) Impacts of the north and tropical Atlantic Ocean on the Antarctic Peninsula and sea ice. *Nature* 505:538–542
- Liebmann B, Smith CA (1996) Description of a complete (interpolated) outgoing longwave radiation dataset. *Bull Amer Meteor Soc* 77:1275–1277
- Massom RA, Scambos TA, Bennetts LG, Reid P, Stammerjohn SE (2018) Antarctic ice shelf disintegration triggered by sea ice loss and ocean swell. *Nature* 558:383–389
- Meehl GA, Arblaster JM, Bitz CM, Chung CTY, Teng H (2016) Antarctic sea-ice expansion between 2000 and 2014 driven by tropical Pacific decadal climate variability. *Nat Geosci* 9:590–595
- Meehl GA, Arblaster JM, Chung CTY, Holland MM, DuVivier A, Thompson L, Yang D, Bitz CM (2019) Sustained ocean changes contributed to sudden Antarctic sea ice retreat in the late 2016. *Nature Comm* 10:14
- Mo KC, Paegle JN (2001) The Pacific-South American modes and their downstream effects. *Int J Climatol* 21:1211–1229
- Mo KC, Higgins RW (1998) The Pacific-South America modes and tropical convection during Southern Hemisphere winter. *Mon Weather Rev* 126:1581–1596
- Power S, Casey T, Folland C, Colman A, Mehta V (1999) Inter-decadal modulation of the impact of ENSO on Australia. *Climate Dynam* 15:319–324
- Parkinson CL (2019) A 40-y record reveals gradual Antarctic sea ice increases followed by decrease at rates far exceeding the rates seen in the Arctic. *Proc Natl Acad Sci USA* 116:14414–14423
- Purich A, Doddridge EW (2023) Record low Antarctic sea ice coverage indicates a new sea ice state. *Commun Earth Environ* 4:314
- Raphael MN (2007) The influence of atmospheric zonal wave three on Antarctic sea ice variability. *J Geophys Res* 112:D12112
- Raphael M, Marshall G, Turner J, Fogt R, Schneider D, Dixon D, Hosking JS, Jones JM, Hobbs WR (2017) The Amundsen Sea Low: variability, change, and impact on Antarctic climate. *Bull Am Meteorol Soc* 97:111–121
- Raphael MN, Handcock MS (2022) A new record minimum for Antarctic sea ice. *Nat Rev Earth Environ* 3:215–216
- Sardeshmukh PD, Hoskins BJ (1988) The generation of global rotational flow by steady idealized tropical divergence. *J Atmos Sci* 45:1228–1251
- Schlosser E, Haumann FA, Raphael MN (2018) Atmospheric influences on the anomalous 2016 Antarctic sea ice decay. *Cryosphere* 12:1103–1119
- Sigmond M, Fyfe JC (2010) Has the ozone hole contributed to increased Antarctic sea ice extent? *Geophys Res Lett* 37:L18502
- Stuecker MF, Bitz CM, Armour KC (2017) Conditions leading to the unprecedented low Antarctic sea ice extent during the 2016 austral spring. *Geophys Res Lett* 44:9008–9019
- Takaya K, Nakamura HA (2001) formulation of a phase independent wave-activity flux for stationary and migratory quasi geostrophic eddies on a zonally varying basic flow. *J Atmos Sci* 58:608–627
- Tetzner D, Thomas E, Allen CA (2019) validation of ERA5 reanalysis data in the Southern Antarctic Peninsula-Ellsworth Land region, and its implications for icecore studies. *Geosciences* 9:289
- Thompson DWJ, Solomon S, Kushner PJ, England MH, Grise KM, Karoly DJ (2011) Signatures of the Antarctic ozone hole in Southern Hemisphere surface climate change. *Nat Geosci* 4:741–749

- Turner J, Phillips T, Marshall GJ, Hosking JS, Pope JO, Bracegirdle TJ, Deb P (2017) Unprecedented springtime retreat of Antarctic sea ice in 2016. *Geophys Res Lett* 44:6868–6875
- Turner J, Holmes C, Harrison TC, Phillips T, Jena B, Reeves-Francois T, Fogt R, Thomas ER, Bajish TCC (2022) Record low Antarctic sea ice cover in February 2022. *Geophys Res Lett* 49:e2022GL098904
- Wang G, Hendon HH, Arblaster JM, Lim E-P, Abhik S, van Rensch P (2019) Compounding tropical and stratospheric forcing of the record low Antarctic sea-ice in 2016. *Nature Comm* 10:13
- Wang J, Luo H, Yang Q, Liu J, Yu L, Shi Q, Han B (2022) An unprecedented record low Antarctic sea-ice extent during austral summer 2022. *Adv Atmos Sci* 39:1591–1597
- Wang S, Liu J, Cheng X, Yang D, Kerzenmacher T, Li X, Hu Y, Braesicke P (2023) Contribution of the deepened Amundsen Sea Low to the record low Antarctic sea ice extent in February 2022. *Environ Res Lett* 18:5
- Yadav J, Kumar A, Mohan R (2022) Atmospheric precursors to the Antarctic sea ice record low in 2022. *Environ Res Commun* 4:12
- Yu L (2019) Global air-sea fluxes of heat, fresh water, and momentum: energy budget closure and unanswered questions. *Ann Rev Mar Sci* 3:227–248
- Yu L, Zhong S, Winkler JA, Zhou M, Lenschow DH, Li B, Wang X, Yang Q (2017) Possible connection of the opposite trends in Arctic and Antarctic sea ice cover. *Sci Rep* 7:45804
- Yu L, Zhong S, Vihma T, Sui C, Sun B (2021) Sea ice changes in the Pacific sector of the Southern Ocean in austral autumn closely associated with the negative polarity of the South Pacific Oscillation. *Geophys Res Lett* 48:e2021GL092409
- Yu L, Zhong S, Sun B (2022a) Synchronous variation patterns of monthly sea ice anomalies at the Arctic and Antarctic. *J Climate* 35:2823–2847
- Yu L, Zhong S, Vihma T, Sui C, Sun B (2022b) Linking the Antarctic sea ice extent changes during 1979–2020 to seasonal modes of Antarctic sea ice variability. *Environ Res Lett* 17:114026
- Yu L, Zhong S, Sui C, Sun B (2023) A regional and seasonal approach to explain the observed trends in the Antarctic sea ice in recent decades. *Int J Climatol* 43:2953–2974
- Zhang JL (2007) Increasing Antarctic sea ice under warming atmospheric and oceanic conditions. *J Climate* 20:2515–2529
- Zhang L, Delworth TL, Yang X, Zeng F, Lu F, Morioka Y, Bushuk M (2022) The relative role of the subsurface Southern Ocean in driving negative Antarctic Sea ice extent anomalies in 2016–2021. *Commun Earth Environ* 3:1
- Zhang C, Li S (2023) Causes of the record-low Antarctic sea-ice in austral summer 2022. *Atmos Ocean Sci Lett*. 16:100353

Publisher's Note Springer Nature remains neutral with regard to jurisdictional claims in published maps and institutional affiliations.

Springer Nature or its licensor (e.g. a society or other partner) holds exclusive rights to this article under a publishing agreement with the author(s) or other rightsholder(s); author self-archiving of the accepted manuscript version of this article is solely governed by the terms of such publishing agreement and applicable law.